Nuclear receptor NR5A2 negatively regulates cell proliferation and tumor growth in nervous system malignancies

Dimitrios Gkikas[a,b], Dimitris Stellas[c], Alexia Polissidis[d], Theodora Manolakou[a], Maroula G. Kokotou[e], George Kokotos[e], and Panagiotis K. Politis[a,1]

[a]Center for Basic Research, Biomedical Research Foundation of the Academy of Athens, 115 27, Athens, Greece; [b]Department of Biology, University of Patras, 265 04, Patras, Greece; [c]Institute of Chemical Biology, National Hellenic Research Foundation, 116 35, Athens, Greece; [d]Centre for Clinical, Experimental Surgery and Translational Research, Biomedical Research Foundation of the Academy of Athens, 11527 Athens, Greece; and [e]Center of Excellence for Drug Design and Discovery, Department of Chemistry, National and Kapodistrian University of Athens, Panepistimiopolis, Athens 15771, Greece

Edited by David D. Moore, University of California, Berkeley, CA, and approved August 9, 2021 (received for review July 19, 2020)

Nervous system malignancies are characterized by rapid progression and poor survival rates. These clinical observations underscore the need for novel therapeutic insights and pharmacological targets. To this end, here, we identify the orphan nuclear receptor NR5A2/LRH1 as a negative regulator of cancer cell proliferation and promising pharmacological target for nervous system–related tumors. In particular, clinical data from publicly available databases suggest that high expression levels of NR5A2 are associated with favorable prognosis in patients with glioblastoma and neuroblastoma tumors. Consistently, we experimentally show that NR5A2 is sufficient to strongly suppress proliferation of both human and mouse glioblastoma and neuroblastoma cells without inducing apoptosis. Moreover, short hairpin RNA–mediated knockdown of the basal expression levels of NR5A2 in glioblastoma cells promotes their cell cycle progression. The antiproliferative effect of NR5A2 is mediated by the transcriptional induction of negative regulators of the cell cycle, *CDKN1A* (encoding for $p21^{cip1}$), *CDKN1B* (encoding for $p27^{kip1}$) and *Prox1*. Interestingly, two well-established agonists of NR5A2, dilauroyl phosphatidylcholine (DLPC) and diundecanoyl phosphatidylcholine, are able to mimic the antiproliferative action of NR5A2 in human glioblastoma cells via the induction of the same critical genes. Most importantly, treatment with DLPC inhibits glioblastoma tumor growth in vivo in heterotopic and orthotopic xenograft mouse models. These data indicate a tumor suppressor role of NR5A2 in the nervous system and render this nuclear receptor a potential pharmacological target for the treatment of nervous tissue–related tumors.

glioblastoma | neuroblastoma | proliferation | LRH1 | agonists

Although nervous system cancers are a heterogeneous group of malignancies with diverse outcomes, many of them are characterized by fast progression and unfavorable prognosis. For example, glioblastoma is a primary neoplasia of the central nervous system (CNS) and one of the most aggressive cancer types (1–5). On the other hand, neuroblastoma is a malignancy of the peripheral nervous system and is less aggressive than glioblastoma but with a very early age of onset during the first years of life. However, a subset of these children belong to the high-risk neuroblastoma patients, from which less than 40% are likely to achieve a long-term cure (6, 7). Despite the dramatic escalation in research efforts and provided therapies, nervous system tumors remain a major cause of mortality worldwide (4, 6, 8–11). These observations underscore the need to identify new target genes and molecular mechanisms that could play a key role in novel therapeutic approaches.

There is strong evidence suggesting that nervous system tumors are originating from neural progenitor/stem cells (NSCs), glial progenitor cells, or glial cells, depending on the tumor context (3, 5, 12–16). Toward the identification of new druggable players in nervous system malignancies, we have previously reported the involvement of nuclear receptor NR5A2 in the regulation of proliferation versus differentiation decisions of NSCs during nervous system development (17). In particular, NR5A2 is sufficient and necessary to suppress cell cycle progression of NSCs, induce differentiation toward the neuronal lineage, and block astrogliogenesis, a property that could be highly relevant to the onset and progression of glioblastoma tumors. In agreement, NR5A2 has been reported to play regulatory roles in embryonic stem cells, embryogenesis, development, and function of many tissues and organs (18–25). Most importantly, although NR5A2 has been previously implicated in tumorigenesis by facilitating either the progression or suppression of different malignancies depending on the cancer cell type (26–38), its role in nervous system tumors remains elusive.

To this end, here, we provide functional evidence suggesting that NR5A2 is involved in the suppression of human and mouse glioblastoma and neuroblastoma cell proliferation. Mechanistically, we show that NR5A2 is both sufficient and necessary for the sustained expression of negative regulators of cell cycle progression in glioblastoma and neuroblastoma cells, including $p21^{Cip1}$, $p27^{Kip1}$, and Prox1. More interestingly, two well-established agonists for NR5A2, dilauroyl phosphatidylcholine (DLPC) and diundecanoyl phosphatidylcholine (DUPC), are able to recapitulate the antiproliferative effect of NR5A2 on glioblastoma cells

Significance

Glioblastomas and neuroblastomas are aggressive cancer types with poor prognosis. Identification of druggable factors that inhibit these tumors will contribute to new therapies. Our data show that nuclear receptor NR5A2 suppresses the growth of glioblastomas and neuroblastomas. This function is facilitated by the ability of NR5A2 to induce critical cell cycle inhibitors including p21, p27, and Prox1. Two small molecule agonists of NR5A2, dilauroyl phosphatidylcholine, and diundecanoyl phosphatidylcholine can mimic its antitumor effect. Our results identify NR5A2 as a potential drug target in nervous system–related cancers.

Author contributions: D.G. and P.K.P. designed research; D.G., D.S., A.P., T.M., M.G.K., G.K., and P.K.P. performed research; D.G. and P.K.P. analyzed data; and D.G. and P.K.P. wrote the paper.

The authors declare no competing interest.

This article is a PNAS Direct Submission.

[1]To whom correspondence may be addressed. Email: ppolitis@bioacademy.gr.

This article contains supporting information online at https://www.pnas.org/lookup/suppl/doi:10.1073/pnas.2015243118/-/DCSupplemental.

Published September 24, 2021.

and wild-type NSCs via the induction of the same critical genes. Most strikingly, treatment with DLPC inhibits glioblastoma tumor growth in vivo in heterotopic and orthotopic xenograft mouse models. Collectively, these observations indicate that NR5A2 negatively regulates tumorigenic properties of glioblastoma and neuroblastoma cells and provide a preclinical proof of concept for the potential use of NR5A2 agonists in the treatment of nervous system malignancies.

Results

NR5A2 Expression Is Associated with Favorable Prognosis in Glioblastoma and Neuroblastoma Patients. To initially address the role of NR5A2 in nervous system tumors, we screened publicly available clinical data from databases such as Oncomine (www.oncomine.org), The Cancer Genome Atlas (TCGA; www.cancergenome.nih.gov), and R2: Genomics Analysis and Visualization Platform (http://r2.amc.nl) for associations between NR5A2 expression levels and various aspects of glioblastoma and neuroblastoma tumors. First, we found that NR5A2 expression levels are significantly reduced in glioblastoma tumors as compared to healthy tissue (Fig. 1*A*). Second, Kaplan-Meier analysis in 348 glioblastoma patients from TCGA via the betastasis database (https://www.betastasis.com/) revealed that high relative expression of NR5A2 is associated with higher survival rates (Fig. 1*B*). Interestingly, similar analysis from another source (https://www.proteinatlas.org/) utilizing TCGA data from 153 glioblastoma patients further confirmed and validated this association (Fig. 1*C*). Likewise, analysis of three different datasets of neuroblastoma patients from R2 genomics analysis and visualization platform suggests a statistically significant correlation between NR5A2 expression and higher survival rates of neuroblastoma patients (Fig. 1 *D*–*F*). These observations are in agreement with our hypothesis that NR5A2 exerts tumor-inhibiting actions in glioblastoma and neuroblastoma cancers.

NR5A2 Overexpression Inhibits the Proliferation of Glioblastoma and Neuroblastoma Cells. To evaluate whether the observed correlation between NR5A2 expression and favorable prognosis in patients has functional importance, we used glioblastoma and neuroblastoma cell lines as a model system to analyze proliferation and apoptosis. We first tested the effect of NR5A2 overexpression on human U87-MG and mouse GL261 glioblastoma cells (Fig. 2). BrdU incorporation assays (with 2 h pulse prior to fixation) revealed a strong reduction in proliferation after NR5A2 overexpression in U87-MG and GL261 cells (Fig. 2 *A*, *B*, and *G*). Furthermore, immunostainings with phosphorylated-histone H3 (pH3) marker revealed a strong reduction in NR5A2-positive glioblastoma cells undergoing mitosis as compared to GFP positive (Fig. 2 *D*, *E*, and *I*). To exclude the possibility of noncell autonomous effects or culture artifacts, we also measured the proliferation rate in the nontransfected cells from the same specimens (same coverslips) (Fig. 2 *A*, *C*, *D*, *F*, *H*, and *J*). In all cases, the untransfected cells in NR5A2 experiments exhibited proliferation rates similar to GFP experiments, confirming that the NR5A2-mediated defect in proliferation is specific for the transfected cells. Similarly, NR5A2 was also sufficient to suppress proliferation of mouse Neuro-2A and human SH-SY5Y neuroblastoma cells in a cell-autonomous manner (Fig. 3 *A*–*J*).

We next investigated whether the low proliferation rates of NR5A2-transfected cells is due to cell death. No evidence of induction of apoptosis was observed in NR5A2-transfected cells as compared to GFP-transfected cells either in glioblastoma or neuroblastoma cells by using two independent assays, immunostainings with an antibody against activated (cleaved) caspase3 (*SI Appendix*, Fig. S1 *A*–*D*), and AnnexinV/7-AAD fluorescence-activated cell sorting analysis (FACS) (*SI Appendix*, Fig. S1*E*). Together, these results show that NR5A2 is potent to inhibit proliferation of glioblastoma and neuroblastoma cells without inducing apoptosis.

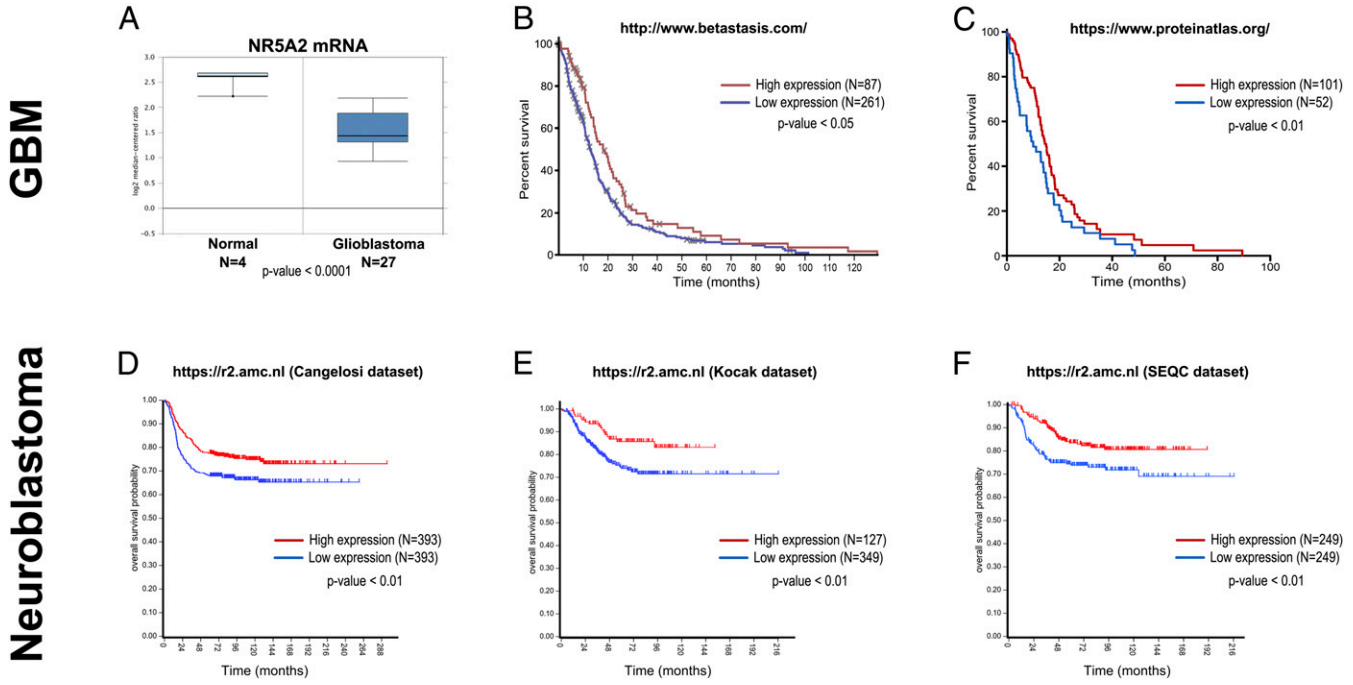

Fig. 1. *NR5A2* expression is correlated with favorable prognosis in glioblastoma and neuroblastoma patients. (*A*) Expression of *NR5A2* mRNA in normal brain tissue and glioblastoma tumor. These data were downloaded from the Oncomine database (https://www.oncomine.org/) and based on the work of Bredel et al. (74); $P < 0.0001$. (*B*) Survival curve (Kaplan-Meier) of glioblastoma patients with relative high and low expression of *NR5A2* from the Betastasis database (https://www.betastasis.com/); $P < 0.05$. (*C*) Survival curve (Kaplan-Meier) of glioblastoma patients with relative high and low expression of *NR5A2* from the Protein Atlas database (https://www.proteinatlas.org/); $P < 0.01$. (*D*–*F*) Survival curves (Kaplan-Meier) of neuroblastoma patients with relative high and low expression of *NR5A2* from R2: Genomics Analysis and Visualization Platform (http://r2.amc.nl) utilizing three different datasets: Cangelosi dataset (*D*), Kocak dataset (*E*), and SEQC dataset (*F*).

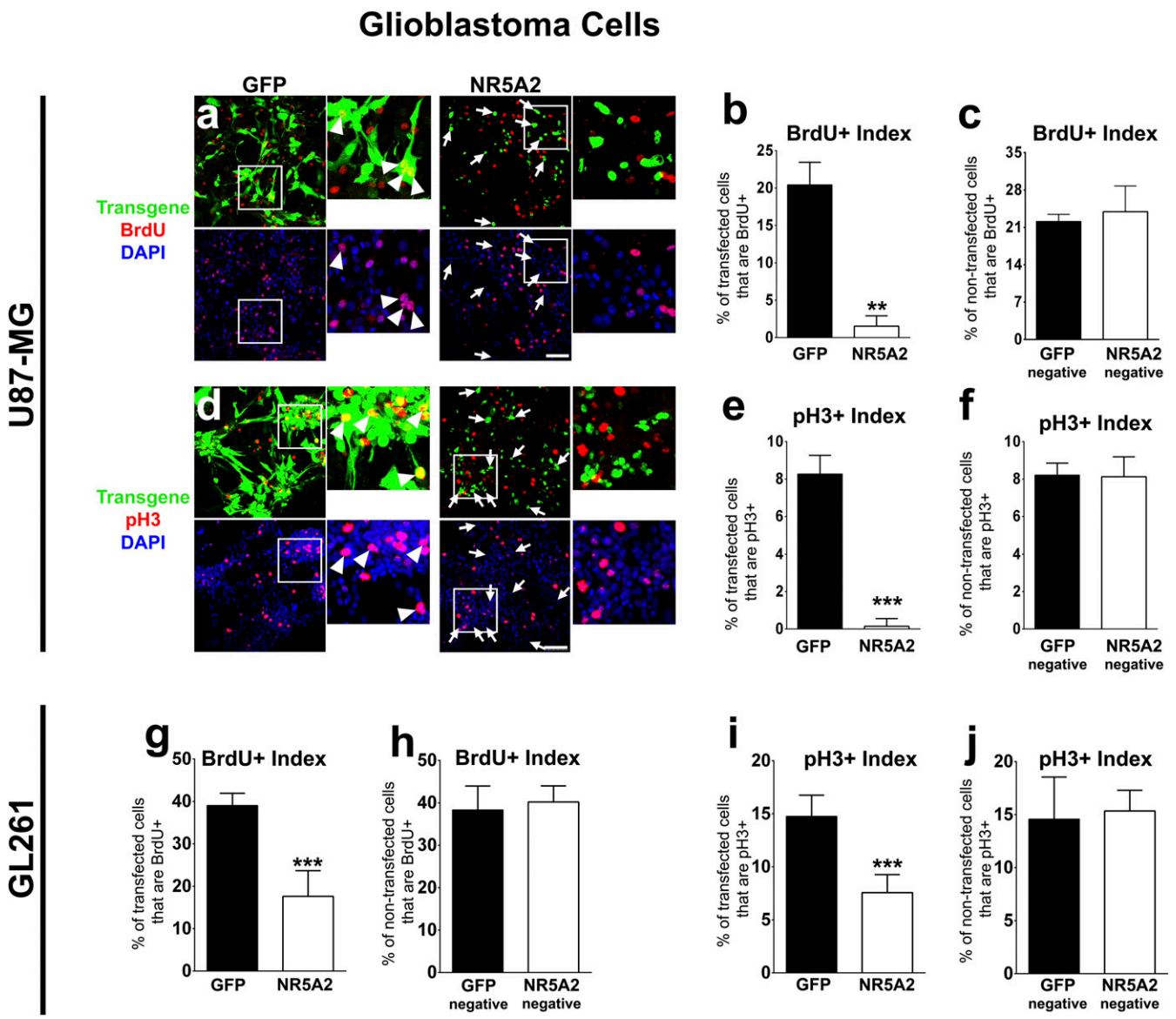

Fig. 2. NR5A2 overexpression inhibits proliferation of human and mouse glioblastoma cells. (*A*) NR5A2 and GFP-transfected U87-MG cells were treated with BrdU for 2 h and then stained with BrdU antibody and DAPI. Larger magnifications of the areas included in the square shapes are presented in the micrographs next to each image. Arrowheads indicate representative double positive cells (GFP positive and BrdU positive). Arrows indicate representative NR5A2-transfected cells that are negative for BrdU. (Scale bar: 75 μM.) (*B*) Quantification of BrdU incorporation in transgene-positive U87-MG cells (GFP: 20.43 ± 3.02%, NR5A2: 1.52 ± 1.38%, $P < 0.01$). (*C*) Quantification of BrdU incorporation in transgene-negative U87-MG cells (GFP: 22.11 ± 1.33%, NR5A2: 23.93 ± 4.81%, $P > 0.1$). (*D*) NR5A2 and GFP-transfected U87-MG cells were immunostained for pH3 and labeled with DAPI. Larger magnifications of the areas included in the square shapes are presented in the micrographs next to each image. Arrowheads indicate representative double positive cells (GFP positive and pH3 positive). Arrows indicate representative NR5A2-transfected cells that are negative for pH3. (Scale bar: 75 μM.) (*E*) Quantification of pH3-positive cells in transgene-positive U87-MG cells (GFP: 8.27 ± 1%, NR5A2: 0.15 ± 0.41%, $P < 0.01$). (*F*) Quantification of pH3-positive cells in transgene-negative U87-MG cells (GFP: 8.21 ± 0.64%, NR5A2: 8.13 ± 1.06%, $P > 0.1$). (*G*) Quantification of BrdU incorporation in transgene-positive GL261 cells (GFP: 39.04 ± 2.88%, NR5A2: 17.62 ± 6.04%, $P < 0.01$). (*H*) Quantification of BrdU incorporation in transgene-negative GL261 cells (GFP: 38.33 ± 5.63%, NR5A2: 40.2 ± 3.8%, $P > 0.1$). (*I*) Quantification of pH3-positive cells in transgene-positive GL261 cells (GFP: 14.76 ± 1.99%, NR5A2: 7.57 ± 1.69%, $P < 0.01$). (*J*) Quantification of pH3-positive cells in transgene-negative GL261 cells (GFP: 14.58 ± 3.96%, NR5A2: 15.35 ± 1.95%, $P > 0.1$). For all cases, $*P < 0.05$, $**P < 0.01$, $***P < 0.001$.

To examine whether the NR5A2-mediated inhibition of cell proliferation is recapitulated under more physiological conditions, we performed xenograft assays in the flanks of NOD/SCID mice. To this end, we utilized a previously constructed and tested adenoviral-based NR5A2 overexpression system (17). We also confirmed here that this system is able to overexpress NR5A2 (Fig. 4*A*) and that adenoviral-overexpressed NR5A2 inhibits cell proliferation in our cells (*SI Appendix*, Fig. S2). Then, SH-SY5Y cells overexpressing either GFP (control condition) or NR5A2 (experimental condition) were transplanted subcutaneously in NOD/SCID mice. The effect of NR5A2 induction in vivo on tumor growth was determined by measuring the volume of tumors every 5 to 8 d (Fig. 3*K*). After 6 wk, the animals were killed, and tumors were photographed and the tumor weight was measured (Fig. 3 *L*–*M*). Remarkably, NR5A2 was sufficient to strongly inhibit the growth of neuroblastoma tumors in NOD/SCID mice.

NR5A2 Induces the Expression of Negative Regulators of the Cell Cycle. Next, we wanted to investigate the molecular mechanism that underlies the antiproliferative action of NR5A2. We have previously

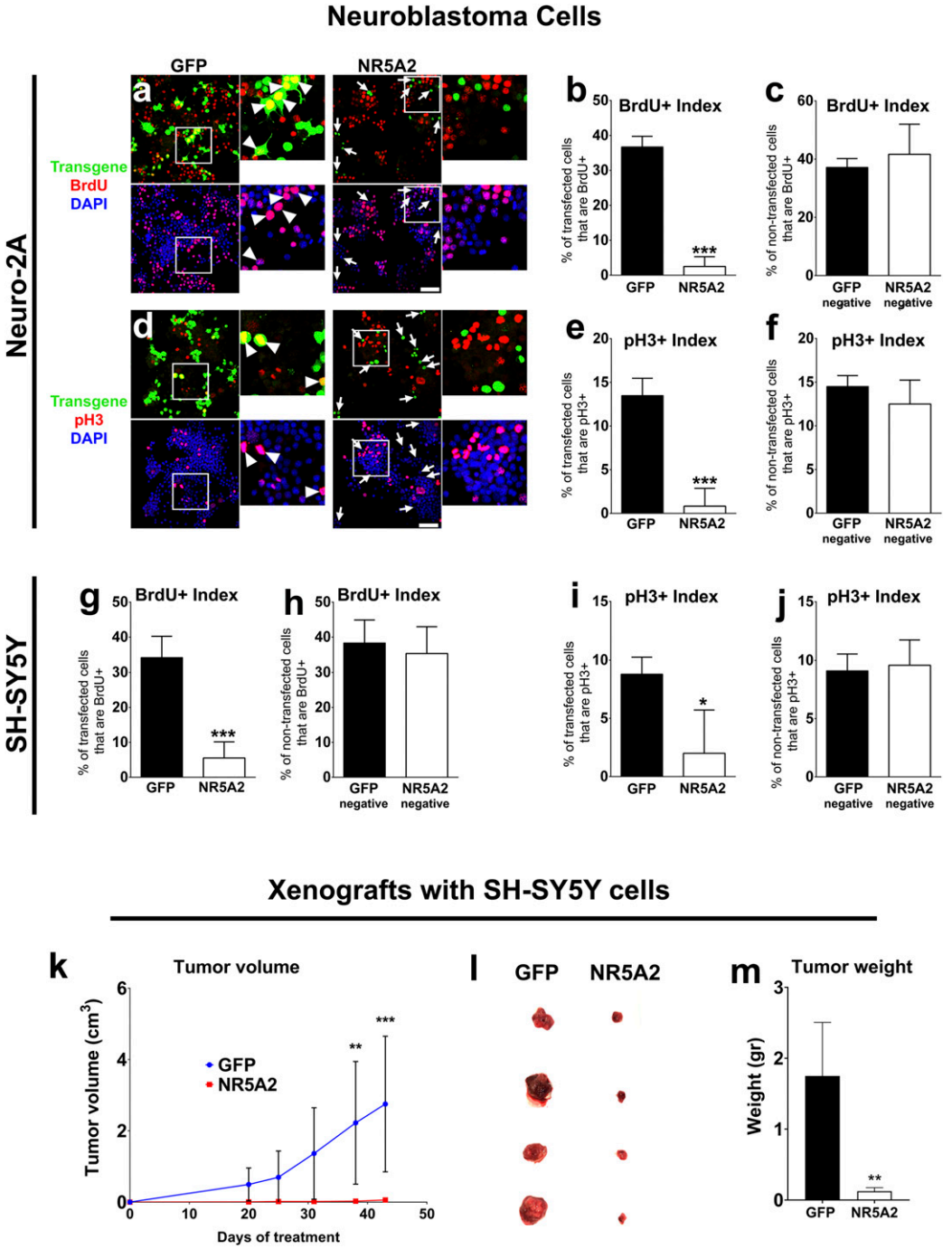

Fig. 3. NR5A2 overexpression inhibits proliferation of human and mouse neuroblastoma cells. (*A*) NR5A2 and GFP-transfected Neuro2A cells were treated with BrdU for 2 h and then stained with BrdU antibody and DAPI. Larger magnifications of the areas included in the square shapes are presented in the micrographs next to each image. Arrowheads indicate representative double positive cells (GFP positive and BrdU positive). Arrows indicate representative NR5A2-transfected cells that are negative for BrdU. (Scale bar: 75 μM.) (*B*) Quantification of BrdU incorporation in transgene-positive Neuro2A cells (GFP: 36.72 ± 3.02%, NR5A2: 2.52 ± 2.78%, $P < 0.01$). (*C*) Quantification of BrdU incorporation in transgene-negative Neuro2A cells (GFP: 37.18 ± 3.04%, NR5A2: 41.67 ± 10.33%, $P > 0.1$). (*D*) NR5A2 and GFP-transfected Neuro2A cells were immunostained for pH3 and labeled with DAPI. Larger magnifications of the areas included in the square shapes are presented in the micrographs next to each image. Arrowheads indicate representative double positive cells (GFP positive and pH3 positive). Arrows indicate representative NR5A2-transfected cells that are negative for pH3. (Scale bar: 75 μM.) (*E*) Quantification of pH3-positive cells in transgene-positive Neuro2A cells (GFP: 13.49 ± 1.99%, NR5A2: 0.83 ± 2.04%, $P < 0.01$). (*F*) Quantification of pH3-positive cells in transgene-negative Neuro2A cells (GFP: 14.51 ± 1.24%, NR5A2: 12.5 ± 2.74%, $P > 0.1$). (*G*) Quantification of BrdU incorporation in transgene-positive SH-SY5Y cells (GFP: 34.28 ± 5.94%, NR5A2: 5.53 ± 4.62%, $P < 0.01$). (*H*) Quantification of BrdU incorporation in transgene-negative SH-SY5Y cells (GFP: 38.33 ± 6.58%, NR5A2: 35.42 ± 7.55%, $P > 0.1$). (*I*) Quantification of pH3-positive cells in transgene-positive SH-SY5Y cells (GFP: 8.79 ± 1.46%, NR5A2: 2 ± 3.7%, $P < 0.01$). (*J*) Quantification of pH3-positive cells in transgene-negative SH-SY5Y cells (GFP: 9.11 ± 1.44%, NR5A2: 9.58 ± 2.14%, $P > 0.1$). (*K–M*) NR5A2 reduces tumor growth in a neuroblastoma xenograft mouse model. (*K*) Quantification of the tumor volume after the subcutaneous transplantation of SH-SY5Y cells overexpressing GFP or NR5A2, as indicated. (*L*) Representative images of whole tumors that were grown in NOD/SCID animals. (*M*) Quantification of the tumor weight of GFP or NR5A2-overexpressing cells (GFP: 1.75 ± 0.755 g, NR5A2: 0.125 ± 0.05 g). For all cases, $*P < 0.05$, $**P < 0.01$, $***P < 0.001$.

shown that, in the context of mouse embryonic NSCs, NR5A2 directly induces the expression of negative regulators of the cell cycle, including cyclin-dependent kinase inhibitors (CDKIs) and Prox1 (17). Since the genes encoding for $p15^{Ink4b}$ and $p16^{Ink4a}$ CDKIs are frequently mutated and not functional in glioblastoma tumors, we tested whether NR5A2 affects the expression of genes encoding for the other two major CDKIs, $p21^{Cip1}$ and $p27^{Kip1}$. To this end, we utilized a previously reported adenoviral-based overexpression system (17) (*SI Appendix*, Fig. S2). Interestingly, overexpression of NR5A2 was able to significantly promote the expression $p21^{Cip1}$ and $p27^{Kip1}$ both at messenger RNA (mRNA) and protein levels (Fig. 4 *A–C* and *E–G*). To test whether this is a specific effect on these CDKIs or a rather general effect due to proliferation block, we measured the expression of many other genes involved in the regulation of cell proliferation. In most cases, NR5A2 overexpression did not affect the expression of all these genes under the same experimental conditions (*SI Appendix*, Fig. S3), except the gene encoding for Cyclin D1 (*CCND1*) (*SI Appendix*, Fig. S3*A*). However, the change in Cyclin D1 appears to be opposite to the cell cycle arrest state of the cells, probably denoting a

feedback response of the cells sensing the need to promote the cell proliferation. Moreover, similar to glioblastoma cells, NR5A2 was also sufficient to enhance the expression of $p21^{Cip1}$ and $p27^{Kip1}$ in human neuroblastoma cells at RNA and protein levels (*SI Appendix*, Fig. S4 *A–C* and *F–H*). In this situation, NR5A2 was additionally able to induce $p16^{Ink4a}$ (*SI Appendix*, Fig. S4*D*), as is also the case in NSCs (17), which is usually inactivated in glioblastoma cells (39–41).

Furthermore, NR5A2 was capable to enhance the expression of Prox1 in both glioblastoma and neuroblastoma cells (Fig. 4*D* and *SI Appendix*, Fig. S4*E*). Interestingly, we and others have previously shown that Prox1 exerts a strong antiproliferative, proneuronal differentiation and anti-astrogliogenic effect on physiological NSCs and neuroblastoma cells (42–44), which is also in good agreement with our observations. Moreover, NR5A2 was sufficient to transactivate the promoters of the genes encoding for CDKIs (Cdkn1a and Cdkn1b) as well as Prox1 (Fig. 4 *H–J*), indicating that NR5A2 acts at the level of transcriptional regulation of all three genes.

Next, to further investigate whether the NR5A2-mediated regulation of all three genes encoding for negative effectors of cell cycle progression (CDKN1A, CDKN1B, and Prox1) is direct, we performed chromatin immunoprecipitation (ChIP) experiments in U87-MG cells. In particular, after ChIP reactions with anti-NR5A2 antibody or control IgG in U87-MG cells, we screened the corresponding gene promoters for NR5A2-binding events by using a series of PCR primer pairs (Fig. 5). Thus, we were able to identify genomic loci close to the transcription start sites of *CDKN1A* (e.g., loc2 and loc3), *CDKN1B* (e.g., loc1 and loc2), and *PROX1* (e.g., loc4 and loc5) genes that were specifically enriched in our ChIP assays for a-NR5A2 reactions as compared to IgG or to other loci in the same genomic regions (Fig. 5). These data suggest that NR5A2-mediated transcriptional regulation of these genes may be through direct interactions with their regulatory sequences.

Then, to assess whether the NR5A2-mediated regulation of $p27^{Kip1}$ (encoded by *Cdkn1b* gene) and Prox1 have functional importance, we performed overexpression experiments for these targets in glioblastoma cells in an attempt to recapitulate the antiproliferative effect of NR5A2. In this direction, we overexpressed $p27^{Kip1}$ or Prox1 in U87-MG cells with GFP overexpression as control (*SI Appendix*, Fig. S5 *A* and *B*). We next checked the proliferative activity of the cells with BrdU incorporation assays and pH3 stainings. Both targets were able to reproduce the negative effect of NR5A2 on cell cycle progression (*SI Appendix*, Fig. S5 *C–J*), suggesting that the ability of NR5A2 to transactivate these genes may explain its strong antiproliferative activity.

Knockdown of NR5A2 Promotes Cell Proliferation. To further study the role of NR5A2 in glioblastoma cells, we asked whether the basal expression levels of NR5A2 in these cells are involved in the regulation of their proliferation properties. To this end, we utilized a validated short hairpin RNA (shRNA) construct specifically targeting the human NR5A2 homolog and one control scrambled shRNA construct based on the lentiviral TRC library (pLKO.1-puro lentiviral vector, Sigma). In particular, we infected U87-MG cells with the indicated lentiviruses and subjected the infected cells in puromycin selection to construct the shNR5A2 and shSCR stable cell lines, respectively (Fig. 6). First, we confirmed that shRNA against NR5A2 was capable to strongly down-regulate the basal expression levels of endogenous NR5A2 as compared to scrambled shRNA (Fig. 6*K*). Then, to analyze the proliferation activity of these stable cell lines, we performed immunofluorescence experiments using Ki67 and pH3 antibodies as proliferation markers. Immunostaining analysis showed that NR5A2 knockdown increases the number of Ki67 and pH3-positive cells (Fig. 6 *A–D*). We next performed FACS analysis to examine proliferation, cell cycle, and cell death using Ki67 and 7-AAD stainings, as previously described by another group (45). The analysis indicated that down-regulation of NR5A2 inhibits the entrance of U87-MG cells in G0 phase (Fig. 6 *E–G*). Consistently, there were more shNR5A2 cycling cells in G1 and S/G2 phases as compared to shSCR cells (Fig. 6 *H* and *I*). Interestingly, down-regulation of NR5A2 was also sufficient to reduce cell death (Fig. 6*J*), which could also contribute to increased proliferation rates. These data further confirm the effect of NR5A2 knockdown on enhancing proliferation of glioblastoma cells. We next tested the expression levels of *CDKN1A* ($p21^{cip1}$) and *CDKN1B* ($p27^{kip1}$) in NR5A2-knockdown cells. Strikingly, down-regulation of NR5A2 resulted in reduced expression of both $p21^{cip1}$ and $p27^{kip1}$ (Fig. 6 *L* and *M*),

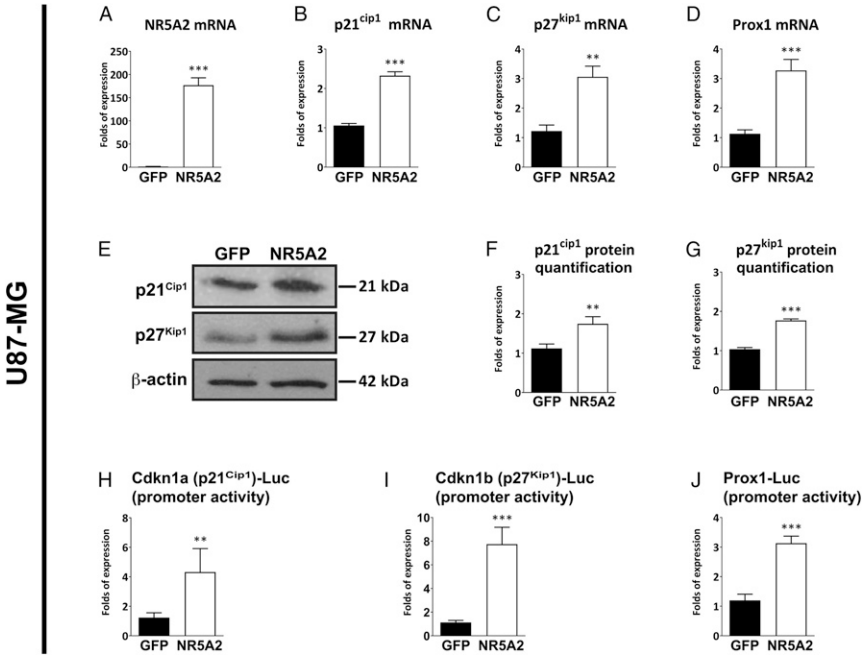

Fig. 4. NR5A2 induces the expression of negative cell cycle regulators in U87-MG cells. (*A*) Overexpression of *NR5A2* in U87-MG cells was measured with real-time RT-qPCR. (*B–D*) Relative expression levels of $p21^{cip1}$ (*B*), $p27^{kip1}$ (*C*), and *Prox1* (*D*) mRNA was measured with quantitative real-time RT-PCR in GFP and NR5A2 overexpression conditions. (*E*) Western blot analysis for $p21^{cip1}$, $p27^{kip1}$, and b-actin proteins in GFP and NR5A2 overexpression conditions. (*F*, *G*) Quantification of protein expression levels of $p21^{cip1}$ (*F*) and $p27^{kip1}$ (*G*) in GFP and NR5A2 overexpression conditions. (*H–J*) Relative promoter activity for $p21^{cip1}$ (*H*), $p27^{kip1}$ (*I*), and *Prox1* (*J*) in GFP and NR5A2 overexpression conditions, measured with luciferase assay. For all cases, $*P < 0.05$, $**P < 0.01$, $***P < 0.001$.

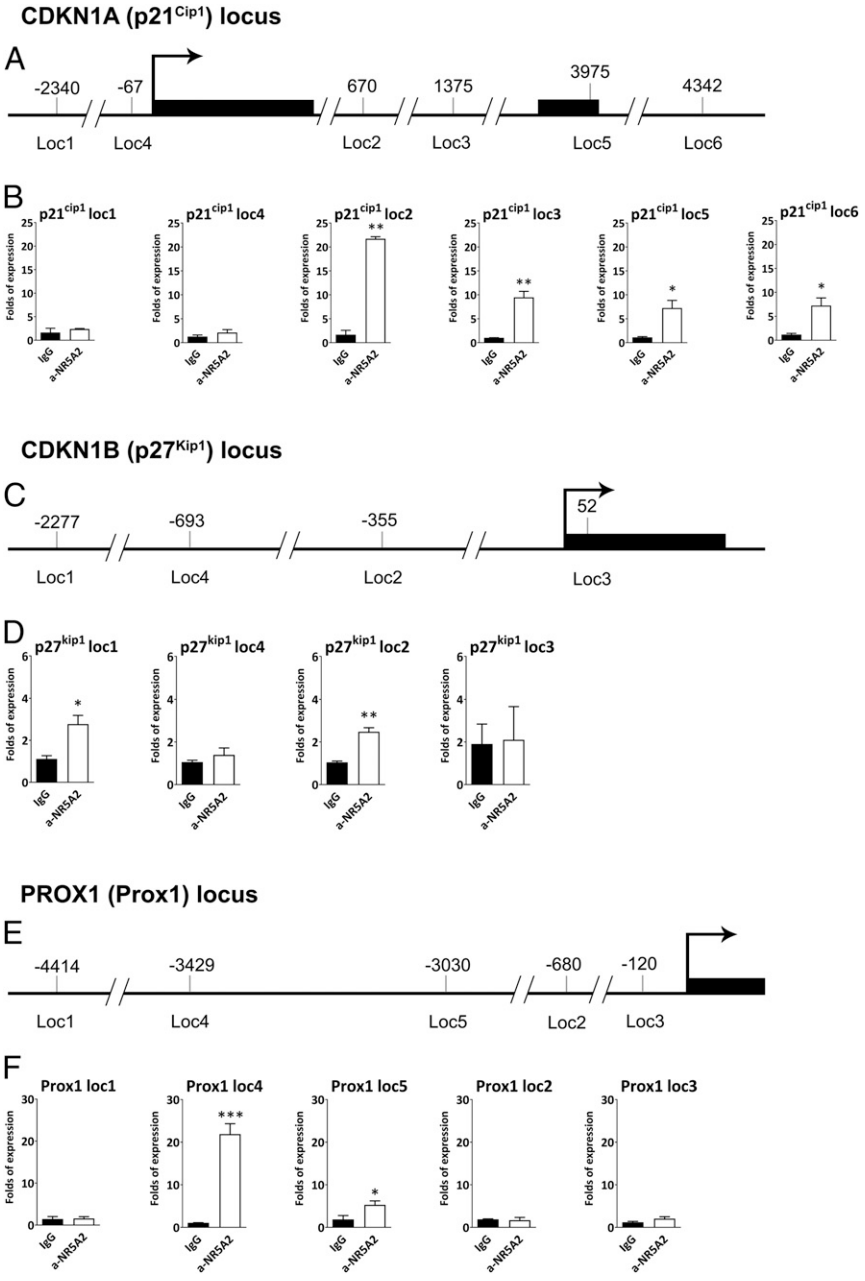

Fig. 5. Endogenous NR5A2 directly interacts with the promoters and regulatory sequences of *CDKN1A* (p21-CIP1), *CDKN1B* (p27-KIP1), and *PROX1* genes in U87-MG cells. (*A*) Schematic representation of the *CDKN1A* gene locus around the transcription start site (TSS; denoted with the broken arrow). The first two exons of *CDKN1A* gene are represented as black boxes. (*B*) ChIP analysis of the binding sites of NR5A2 to *CDKN1A* gene locus. ChIP experiments were performed using anti-NR5A2 antibody (a-NR5A2) or a control antibody (IgG) in chromatin isolated from wild-type U87-MG cells. For a-NR5A2 and IgG reactions, the same amount of DNA was used as a template. The primer pairs used to amplify the corresponding DNA sequences are indicated with specific loci numbers below the schematic drawing in *A*. Numbers above the schematic drawing denote the distance from the TSS. Note that NR5A2 specifically binds to the loci loc2 and loc3 as well as loc5 and loc6 but less efficiently than the first two. (*C*) Schematic representation of the *CDKN1B* gene locus around the TSS. The first exon of *CDKN1B* gene is represented as a black box. (*D*) ChIP analysis of the binding sites of NR5A2 to *CDKN1B* gene locus, as described for *CDKN1A* gene. The primer pairs used to amplify the corresponding DNA sequences are indicated with specific loci numbers below the schematic drawing in *C*. Numbers above the schematic drawing denote the distance from the TSS. Note that NR5A2 specifically binds to loc1 and loc2. (*E*) Schematic representation of the *Prox1* gene locus around the TSS. The first exon of *Prox1* gene is represented as a black box. (*F*) ChIP analysis of the binding sites of NR5A2 to *Prox1* gene locus, as described for *CDKN1A* gene. The primer pairs used to amplify the corresponding DNA sequences are indicated with specific loci numbers below the schematic drawing in *E*. Numbers above the schematic drawing denote the distance from the TSS. Note that NR5A2 specifically binds to loc4 and less efficiently to loc5. For all cases, $*P < 0.05$, $**P < 0.01$, $***P < 0.001$.

which is the opposite effect of NR5A2 overexpression, suggesting that NR5A2 is both sufficient and necessary for the proper expression of these genes.

Subsequently, we wanted to examine whether overexpression of the downstream targets of NR5A2 in glioblastoma cells can rescue the over-proliferative phenotype of shNR5A2 cells. To this end, we overexpressed the $p27^{kip1}$ CDKI and Prox1 in the stable cell lines that express the shNR5A2 or scrambled shRNAs and then measured the proliferation capacity of the transfected cells. Interestingly, only $p27^{kip1}$ was sufficient to significantly rescue the overproliferative phenotype of shNR5A2 cells (*SI Appendix*, Fig. S6). This finding is consistent with the importance of CDKIs in cell cycle regulation as well as with the hypothesis that $p27^{kip1}$ is directly regulated by NR5A2 to mediate an antiproliferative action via direct interactions of $p27^{kip1}$ with cyclins/CDK complexes. On the other hand, Prox1 could not rescue the antiproliferative phenotype of shNR5A2, in agreement with the previously reported observations that Prox1 and NR5A2 directly interact at the protein level to mediate a number of cellular events (17, 42, 44). Therefore, in this case, we favor a scenario that first NR5A2 up-regulates Prox1, then they form a protein complex, and the formation of this complex is required for the antiproliferative function of Prox1.

Taken together, our observations suggest that NR5A2 is sufficient and necessary to suppress the tumorigenic properties of glioblastoma cells and render it a potential target for new therapeutic approaches.

Small Molecule Agonists of NR5A2 Mimic Its Role in Wild-Type NSCs and Glioblastoma Cells. Although natural ligands for nuclear receptor NR5A2 are elusive, in the last few years, a number of small molecule agonists have been developed that are capable of binding its LBD domain and enhancing its activity as a transcription factor (46–49). These compounds were developed to

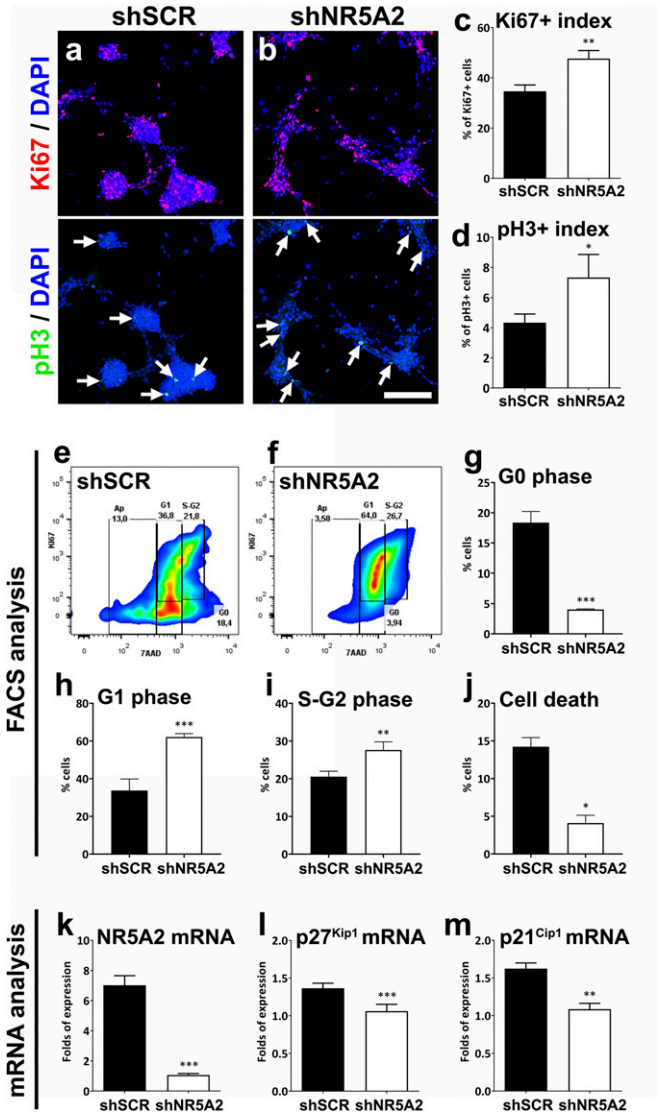

Fig. 6. shRNA-mediated down-regulation of NR5A2 induces proliferation of U87-MG cells. (*A*, *B*) Stable U87-MG cells carrying either the scrabble shRNA construct (shSCR) or shRNA targeting human *NR5A2* (shNR5A2) were stained for Ki67 (red), pH3 (green), and DAPI (blue), as indicated. Arrows denote representative cells that are positive for the pH3 marker in shSCR or shNR5A2 stable cell lines. Note that pH3-positive cells are more abundant in the shNR5A2 cells. (Scale bar: 75 μM.) (*C*) Quantification of Ki67-positive cells in shSCR and shNR5A2 conditions (shSCR: 34.67 ± 2.52%, shNR5A2: 47.67 ± 3.21%). (*D*) Quantification of pH3-positive cells in shSCR and shNR5A2 conditions (shSCR: 4.33 ± 0.58%, shNR5A2: 7.33 ± 1.53%). Arrows indicate the pH3 positive cells. (*E*, *F*) Graphical representation of FACS cell cycle analysis for shSCR and shNR5A2 U87-MG cells with Ki67 and 7-AAD staining. (*G–J*) Percentage of cells present in different phases of cell cycle and cell death for shSCR and shNR5A2 U87-MG cells, as indicated. (*K–M*) Relative expression levels of *NR5A2* (confirmation of shRNA-mediated down-regulation of *NR5A2*) and $p21^{cip1}$ and $p27^{kip1}$ mRNA in shSCR and shNR5A2 conditions, measured with quantitative real-time RT-PCR. For all cases, $*P < 0.05$, $**P < 0.01$, $***P < 0.001$.

promote the antilipidemic and antidiabetic properties of NR5A2 (47, 50) and have not been previously reported to function in cells of the nervous system. To initially investigate whether these compounds can be used to reduce glioblastoma tumor growth, we tested the ability of two well-established agonists for NR5A2, DLPC, and DUPC to mimic the effect of NR5A2 on wild-type NSCs and glioblastoma U87-MG cells. These experiments could provide an initial proof of concept that the NR5A2 agonists are effective in the context of the nervous system. Accordingly, we first treated NSCs, isolated from embryonic mouse forebrain, with two different concentrations of DLPC and DUPC (50 and 100 μM), whereas as a control experiment, we treated the cells with ethanol, which was the solvent of the two phosphatidilcholines. Both compounds were able to reduce proliferation of NSCs in a dose-dependent manner (*SI Appendix*, Fig. S7 *A–L*), as indicated by BrdU incorporation assays and pH3 immunostainings. In our previously published work, we have shown that NR5A2 functions to promote neuronal differentiation and suppress astrogliogenesis in NSCs (17). To examine whether these compounds can also enhance the differentiation properties of NR5A2 in NSCs, we treated these cells with DLPC and DUPC and let them differentiate by withdrawing the growth factors (fibroblast growth factor [FGF] and epidermal growth factor [EGF]) from the culture medium. In this case, DLPC was able to faithfully recapitulate these properties by inducing the neuronal marker (TuJ1) and down-regulating the astrocytic marker (GFAP) in a dose-dependent manner (*SI Appendix*, Fig. S7 *M–X*). On the other hand, DUPC exerted similar actions but was not as efficient as DLPC in promoting neuronal differentiation (*SI Appendix*, Fig. S7 *M–X*). Next, we tested the ability of both agonists to suppress proliferation of glioblastoma U87-MG cells. We have chosen to test the agonists in these cells due to the observation that we were able to detect basal expression levels of NR5A2 in U87-MG at both mRNA and protein levels as compared to other cells (e.g., SH-SY5Y neuroblastoma cells) (*SI Appendix*, Fig. S8). Similar to NSCs, both agonists were sufficient to suppress proliferation of glioblastoma cells (Fig. 7 *A–L*), with DLPC following a concentration-dependent reduction of BrdU incorporation and pH3 immunostaining. Both agonists were not able to induce apoptosis or cell death in glioblastoma cells, as shown by annexin V/7-AAD FACS analysis (*SI Appendix*, Fig. S1*F*). Furthermore, DLPC was also able to mimic the effects of NR5A2 on gene regulation by inducing the expression levels of *CDKN1A* ($p21^{cip1}$), *CDKN1B* ($p27^{kip1}$), and *Prox1* at the concentration of 100 μM (Fig. 7 *M–O*). Collectively, these observations show a strong antiproliferative action of NR5A2 agonists in NSCs and glioblastoma cells.

NR5A2 Knockdown Rescues the Antiproliferative Effect of DLPC. To examine whether the antiproliferative effect of DLPC is specific and mediated via enhancement of NR5A2 transcriptional activity, we performed the DLPC treatment in the context of an shNR5A2 stable cell line and compared it to the control shSCR-U87-MG cells. We investigated the proliferative activity of these stable cell lines in the presence of the ligand of NR5A2, DLPC, at the concentration of 100 μM. We used ethanol treatment as a control experiment (vehicle) in both shNR5A2 and shSCR U87-MG cells. For the quantification of cell proliferation, we implemented Ki67 and pH3 immunostainings. Interestingly, while DLPC-treated shSCR cells showed reduced numbers of proliferation indices (Ki67 and pH3) as compared to ethanol-treated cells, this reduction was abolished in the shNR5A2 cells (*SI Appendix*, Fig. S9). Moreover, in all cases, shNR5A2 cells exhibited higher proliferation indices as compared to shSCR, further confirming the requirement of NR5A2 for suppressing proliferation of glioblastoma cells (*SI Appendix*, Fig. S9). These observations indicate a specific action of DLPC via NR5A2, which is lost when knockdown of NR5A2 is applied.

DLPC Suppresses Tumor Growth In Vivo. Then, we examined if DLPC has the same tumor suppression effect on an in vivo model. First, we performed experiments with DLPC in a heterotopic xenograft mouse model because the ability of DLPC to cross the blood-brain barrier (BBB) has not been previously examined. To this end, we subcutaneously transplanted U87-MG cells in NOD/SCID mice. After 13 d, when the tumors were detectable and measurable, we treated the mice with a daily dose of 100 mg/kg of DLPC. The

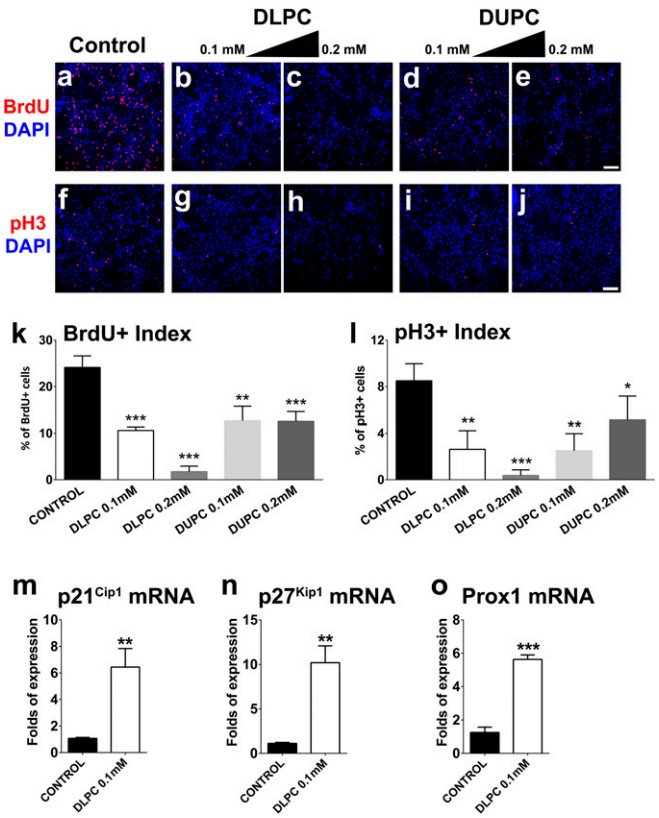

Fig. 7. NR5A2 agonists (DLPC and DUPC) suppress proliferation of U87-MG cells. (*A–E*) U87-MG cells were treated with two concentrations of DLPC and DUPC, incubated with BrdU for 2 h and then labeled with BrdU antibody and DAPI. (Scale bar: 75 μM.) (*F–J*) U87-MG cells were treated with two concentrations of DLPC and DUPC and then stained for pH3 and DAPI. (Scale bar: 75 μM.) (*K*) Quantification of BrdU incorporation in ethanol (control) and DLPC and DUPC-treated U87-MG cells (control: 24.13 ± 2.5%, DLPC 0.1 mM: 10.64 ± 0.75%, DLPC 0.2 mM: 1.75 ± 1.19%, DUPC 0.1 mM: 12.63 ± 3.15% DUPC 0.2 mM: 12.5 ± 2.12%). (*L*) Quantification of pH3-positive cells in ethanol (control) and DLPC and DUPC-treated U87-MG cells (control: 8.5 ± 1.47%, DLPC 0.1 mM: 2.64 ± 1.6%, DLPC 0.2 mM: 0.38 ± 0.48%, DUPC 0.1 mM: 2.5 ± 1.47%, DUPC 0.2 mM: 5.13 ± 2.06%.). (*M*) Relative expression levels of $p21^{cip1}$, $p27^{kip1}$, and *Prox1* mRNA in ethanol and DLPC (0.1 mM) treated U87-MG cells, measured with quantitative real-time RT-PCR. For all cases, $*P < 0.05$, $**P < 0.01$, $***P < 0.001$.

control group was treated with the solvent (vehicle), which was 30% propylene glycol and 10% ethanol. In order to keep a record for tumor growth, we measured their volume every 4 to 5 d. Most importantly, after 13 d of treatment, DLPC was sufficient to suppress tumor growth in NOD/SCID mice, with the average volume of treated tumors to be two times smaller than the volume of control tumors (Fig. 8 *A–C*). We next performed immunostainings for Ki67 and pH3 to evaluate the proliferation ability of glioblastoma cells in these tumors. Treatment with DLPC significantly reduced the number of Ki67-positive and pH3-positive cells in the tumor section (Fig. 8 *D* and *E*). Specifically, quantification of Ki67 and pH3 indices in the control group (vehicle) was about three times higher than in DLPC-treated tumors (Fig. 8 *I* and *J*). Similarly, immunostainings of the tumors with antibodies against Nestin and Vimentin showed that DLPC reduces both markers (Fig. 8 *F*, *G*, *K*, and *L*), indicating a decrease in the neural stem cellness and EMT capacity, respectively. In addition, these changes in tumor aggressiveness after treatment with DLPC are not followed by an induction of apoptosis (Fig. 8 *H* and *M*), also confirming our in vitro analysis (*SI Appendix*, Fig. S1*F*).

Finally, we wanted to investigate if DLPC is able to inhibit glioblastoma tumor growth in an orthotopic xenograft mouse model. To this end, we first tested whether DLPC can cross the BBB and activate NR5A2 in the brain. To demonstrate this, we developed an experimental method for DLPC detection and determination by liquid chromatography-high resolution mass spectrometry (LC-HRMS) (*SI Appendix*, Fig. S10*A*). By using this method, we were able to detect an increase in DLPC concentration in the brain of the treated mice as compared to untreated animals. In particular, we treated adult mice with DLPC or vehicle for 3 d, then we isolated the brain and prepared cell lysates for LC-HRMS. *SI Appendix*, Fig. S10*A* shows the extracted ion chromatogram (EIC) of DLPC in a standard solution, while EICs of representative brain samples of DLPC-treated and vehicle-treated animals are presented in *SI Appendix*, Fig. S10 *B* and *C*, respectively. Quantification of these data from three independent experiments (biological replicates) indicates that the concentration of DLPC in the brain of DLPC-treated animals is significantly higher than that of the vehicle-treated ones (*SI Appendix*, Fig. S10*D*). These data suggest that DLPC is probably able to cross the BBB.

To further confirm this observation, we examined whether DLPC can affect expression of NR5A2 downstream target genes as well as genes encoding for NSC markers, such as *Sox2* and *Nestin*, in the whole brain or the adult dentate gyrus (DG) of the hippocampus. Thus, we isolated total RNA from the whole brain or specifically from the DG (a brain region where adult NSCs are found) of the DLPC-treated or vehicle-treated animals and tested the expression of downstream target genes of NR5A2. We decided to focus on the DG because we have recently shown that NR5A2 is expressed in this neurogenic brain region (51). Interestingly, DLPC was able to induce *Cdkn1a* ($p21^{cip1}$) and *Cdkn1b* ($p27^{kip1}$) genes in the whole brain as well as in the DG of DLPC-treated mice (*SI Appendix*, Fig. S10 *E*, *F*, *I*, *J*, *M*, and *N*). In addition, two well-established downstream target genes of NR5A2, namely *Cyp7a1* and *Cyp8b1* (47, 52), are also induced in the brain of DLPC-treated mice (*SI Appendix*, Fig. S10 *G* and *H*), further implying that DLPC crosses the BBB and transactivates all these genes in the brain and/or DG. Moreover, in the DG, DLPC is also sufficient to reduce the expression of the NSC markers Nestin and Sox2 (*SI Appendix*, Fig. S10 *K*, *L*, *M*, and *O*), which is also consistent with an NR5A2-mediated antiproliferative action of DLPC in this niche of adult neural progenitor cells.

Next, to test the antitumorigenic properties of DLPC in a more physiologically relevant context, we established an orthotopic xenograft mouse model. In particular, stereotactic injection of U87-MG cells into the brain parenchyma of NOD/SCID mice was sufficient to generate large glioblastoma tumors within 5 wk after injection (Fig. 9*A*). Most importantly, oral administration of DLPC for 3 wk, starting 2 wk after cell injection, inhibits the growth of glioblastoma tumors in the mouse brain (Fig. 9 *B* and *C*). Consistently, the tumors from DLPC-treated animals exhibit reduced levels of proliferation markers, such as Ki67 and pH3 (Fig. 9 *D* and *E*), which is indicative of low growth capacity, as well as reduced expression of Vimentin, an EMT marker. Similar to the heterotopic xenograft assays and in vitro experiments in glioblastoma cells, treatment with DLPC did not induce apoptosis (Fig. 9 *D* and *E*) despite the reduction in proliferation rates. Conclusively, our observations suggest that DLPC is able to impair the growth of glioblastoma tumors in the mouse brain.

Collectively, these results render NR5A2 as a promising drug target for glioblastoma treatment.

Discussion

Analysis of the publicly available clinical data from TCGA and Oncomine databases and R2 genomics analysis and visualization platform suggests that high expression levels of nuclear receptor NR5A2 are associated with favorable prognosis in glioblastoma

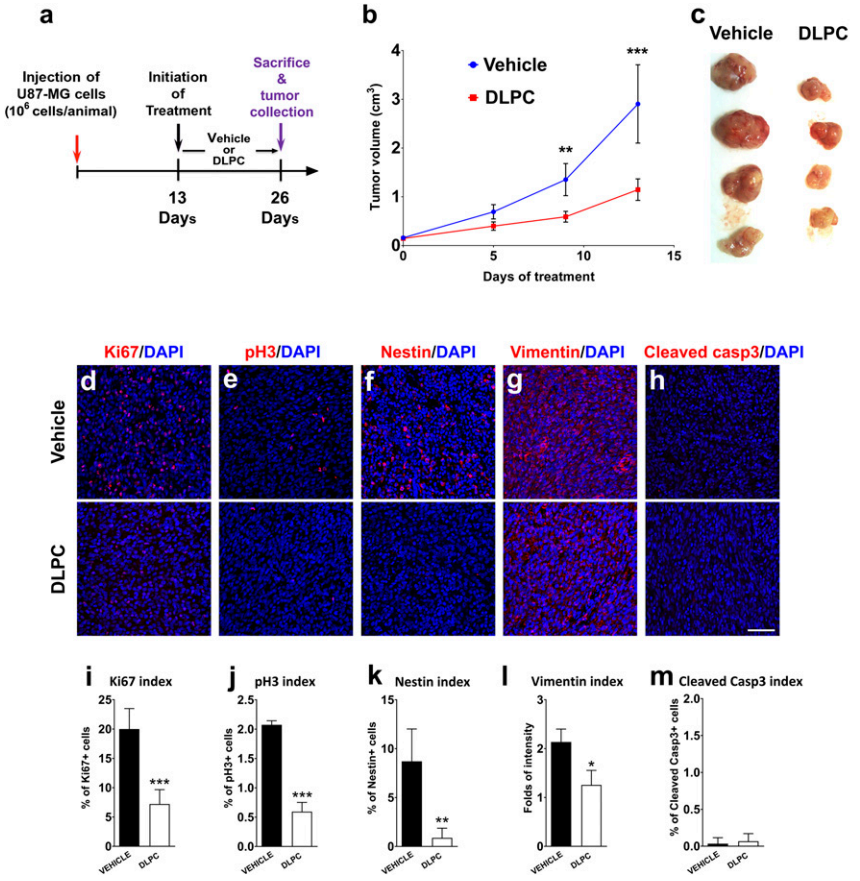

Fig. 8. DLPC reduces glioblastoma tumor growth in a heterotopic allotransplantation mouse model. (*A*) Schematic representation of the experimental design. In particular, 1×10^6 U87-MG cells were injected into the flanks of NOD/SCID adult mice. Tumors were allowed to grow for 13 d. Then, the animals were randomly divided into two groups. One group was treated with vehicle and the other group with DLPC (oral administration with gavage, a daily dose of 100 mg of DLPC per kilogram of mouse weight). After 13 d of treatment, animals were killed and the tumors were collected, photographed, and processed for histological preparations. (*B*) Quantification of the volume of tumor every 4 to 5 d after the initiation of treatment (day 0) with DLPC or Vehicle, as indicated, in NOD/SCID mice that have been inoculated with U87-MG in the flanks. (*C*) Representative images of whole tumors that were grown in NOD/SCID animals after U87-MG cell injections and treatment with vehicle or DLPC. The tumor images were taken at the end of the experiment, e.g., 13 d after the initiation of treatment. (*D*) Labeling of tumor sections for Ki67 and DAPI. The tumors were collected at the end of the experiment, 13 d after the initiation of DLPC or vehicle treatment. (*E*) Labeling of tumor sections for pH3 and DAPI. The tumors were collected at the end of the experiment, 13 d after the initiation of DLPC or vehicle treatment. (*F*) Labeling of tumor sections for Nestin and DAPI. The tumors were collected at the end of the experiment, 13 d after the initiation of DLPC or vehicle treatment. (*G*) Labeling of tumor sections for Vimentin and DAPI. The tumors were collected at the end of the experiment, 13 d after the initiation of DLPC or vehicle treatment. (*H*) Labeling of tumor sections for activated caspase3 and DAPI. The tumors were collected at the end of the experiment, 13 d after the initiation of DLPC or vehicle treatment. (*I*) Quantification of the Ki67 index in the vehicle and DLPC-treated tumors (vehicle: 20 ± 3.5%, DLPC: 7.21 ± 2.46%). (*J*) Quantification of the pH3 index in the vehicle and DLPC-treated tumors (vehicle: 2.08 ± 0.07%, DLPC: 0.56 ± 0.16%). (*K*) Quantification of the Nestin index in the vehicle and DLPC-treated tumors (vehicle: 8.714 ± 3.302%, DLPC: 0.875 ± 0.991%). (*L*) Quantification of the Vimentin index in the vehicle and DLPC-treated tumors (vehicle: 2.196 ± 0.264, DLPC: 1.257 ± 0.297). (*M*) Quantification of the cleaved caspase3 index in the vehicle and DLPC-treated tumors (vehicle: 0.033 ± 0.081%, DLPC: 0.066 ± 0.1%). (For all micrographs, *C*–*G*, scale bar: 50 μM.) For all cases, $*P < 0.05$, $**P < 0.01$, $***P < 0.001$.

and neuroblastoma patients. Consistently, we have previously revealed a strong antiproliferative and antigliogenic effect of NR5A2 on wild-type neural progenitor cells of the nervous system (17). These observations raised the hypothesis that NR5A2 may exert a tumor-suppressive function in glioblastoma and other nervous system–related cancers. Indeed, here, we show that NR5A2 strongly inhibits the tumorigenic properties of glioblastoma and neuroblastoma cells, whereas endogenous basal expression levels in glioblastoma cells are necessary for suppressing the progression of the cell cycle. Most interestingly, NR5A2 is a druggable orphan nuclear receptor with well-established small molecule agonists (47, 48, 53–55). Some of the most well-characterized agonists for NR5A2 are DLPC and DUPC phospholipids and are able to efficiently promote the induction of its downstream target genes (47, 56). DLPC has a good oral bioavailability and is listed in the Food and Drug Administration (FDA) substance registration system (UNII-31NE1DVE91) (57). However, prior to our study, the translational research interest regarding NR5A2 agonists was mainly focused on other tissues and pathological conditions, such as diabetes, cholesterol metabolism, atherosclerosis, and liver diseases (47, 55, 58). The antiproliferative action of NR5A2 in glioblastoma cells posed the question of whether NR5A2 agonists can recapitulate this action in vitro and in vivo. To this end, here, we show that DLPC and DUPC can mimic the antiproliferative effect of NR5A2 on wild-type NSCs and human glioblastoma cells. In the context of NSCs, both agonists are also able to inhibit astrogliogenesis and induce neuronal differentiation, further supporting an antiglioblastoma action. In agreement with these observations, DLPC strongly suppresses the growth of glioblastoma tumors in vivo in heterotopic and orthotopic NOD/SCID xenograft mouse models. Therefore, these data provide a preclinical proof of concept for further investigation into the usage of NR5A2 agonists in novel therapeutic approaches for glioblastoma cancer. Considering that many new small molecule agonists for NR5A2 have been recently discovered (47, 48, 53–55), it would be extremely interesting to test them in the context of nervous system–related tumors. Moreover, the ability of DLPC and DUPC to enhance neurogenesis in ex vivo cultured NSCs and the observation that DLPC crosses the BBB may also indicate that these agonists could be useful in future applications of regenerative medicine against neurodegenerative and neurological diseases.

Furthermore, to address the question of which downstream targets mediate the strong antiproliferative effect of NR5A2 on glioblastoma and neuroblastoma cells, we focused on key inhibitors of G1/S phase progression. The observation that NR5A2 overexpression in U87-MG cells completely blocks incorporation of BrdU (Fig. 2 *A*–*F*) suggested that these cells were probably stalled in G1/G0 and unable to enter the S phase, when BrdU is incorporated into the DNA. Therefore, we propose that NR5A2 may be directly involved in the cell-type specific mechanisms that negatively control the progression of cell cycle from G1 to S phase. Consistently, here, we provide evidence that NR5A2 acts on suppressing cell cycle progression by inducing a number of key inhibitors of G1/S phase progression in glioblastoma and neuroblastoma cells, including the CDK inhibitors $p21^{Cip1}$ and $p27^{Kip1}$ as well as

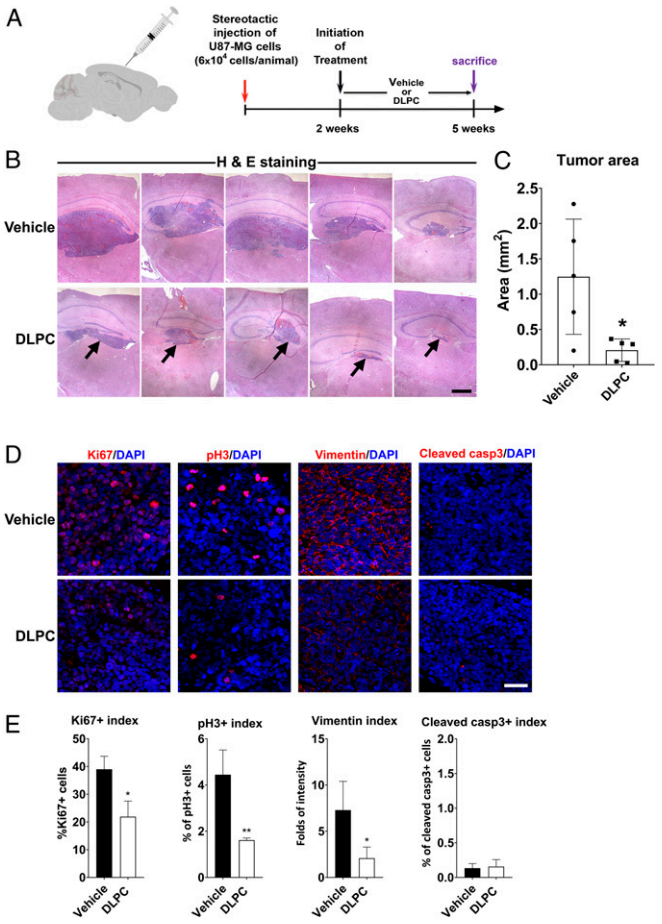

Fig. 9. DLPC suppresses glioblastoma tumor growth in an orthotopic allotransplantation mouse model. (*A*) Schematic representation of the experimental design. In particular, 60,000 U87-MG cells were stereotactically injected into the brain parenchyma of NOD/SCID adult mice. Tumors were allowed to grow for 2 wk. Then, the animals were randomly divided into two groups. One group was treated with vehicle and the other group with DLPC (oral administration with gavage, a daily dose of 100 mg of DLPC per kilogram of mouse weight). After 3 wk of treatment, animals were killed and the brains were processed for histological preparations. (*B*) Hematoxylin–eosin (H&E) stainings of representative coronal sections from the brain of vehicle-treated or DLPC-treated animals. Each micrograph corresponds to the largest part of the tumor from each different animal ($n = 5$ biological replicates). The brains were serially sectioned, and the sections representing the peak of each tumor size were selected and included in the image. Tumors are visible as a compact mass of cells stained with dark blue color. Arrows in the lower panel indicate the presence of tumors in DLPC-treated mice. (*C*) Quantification of the tumor area in the vehicle and DLPC-treated animals (vehicle: 1.25 ± 0.82 mm^2, DLPC: 0.21 ± 0.16 mm^2). (*D*) Labeling of tumor sections for Ki67/DAPI, pH3/DAPI, Vimentin/DAPI, and cleaved caspese3/DAPI, as indicated. (Scale bar: 40 μM.) (*E*) Quantification of the Ki67 (vehicle: 39 ± 4.7%, DLPC: 21.89 ± 5.64%), pH3 (vehicle: 4.44 ± 1.07%, DLPC: 1.61 ± 0.1%), Vimentin (vehicle: 7.29 ± 3.1, DLPC: 2.08 ± 1.2), and cleaved caspase3 (vehicle: 0.13 ± 0.067%, DLPC: 0.16 ± 0.1%) indices in the vehicle and DLPC-treated tumors, as indicated. For all cases, $*P < 0.05$, $**P < 0.01$, $***P < 0.001$.

Prox1, a transcription regulator with antiproliferative actions in the nervous system (32, 42, 59–63). Interestingly, treatment of glioblastoma cells with DLPC significantly promotes the expression of all three downstream target genes. On the other hand, overexpression of $p27^{Kip1}$ and Prox1 in the same cellular system was sufficient to recapitulate the strong antiproliferative effect of NR5A2, further supporting our hypothesis that these players may mediate the NR5A2 action. In addition, NR5A2 appears to control the expression of $p21^{Cip1}$, $p27^{Kip1}$, and Prox1 not only at the protein and transcriptional level but also at the promoter transactivation level, possibly through direct binding to the regulatory sequences of these genes. This binding was further confirmed with ChIP experiments. However, based on our observations, we cannot totally rule out the possibility of an additional indirect mode of regulation. Along these lines, we have previously shown that NR5A2 directly binds on and transactivates Prox1 promoter in NSCs (17) and that Prox1 is also able to directly activate the promoter of the *CDKN1B* gene encoding for $p27^{Kip1}$ (42). These data imply that NR5A2-mediated transactivation of $p27^{Kip1}$ may be mediated by Prox1. Moreover, based on our data, we cannot exclude additional actions of NR5A2 in other genes that may also contribute to its strong antiproliferative effect on glioblastoma and neuroblastoma cells.

Similar to the nervous system, it has been previously shown that NR5A2 exerts antitumorigenic actions in the pancreas. Specifically, genome-wide association studies have found a number of pancreatic adenocarcinoma-linked SNPs, which are localized either over or in close proximity to the *NR5A2* gene (64, 65), suggesting that mutations or genetic variations in the *NR5A2* gene locus may function as risk factors for pancreatic cancer. In agreement, heterozygosity or pancreas-specific loss of *NR5A2* dramatically sensitizes the pancreas to oncogenic Kras-driven intraepithelial neoplasia in a mouse model (31, 65, 66). Moreover, it was shown that this tumor-inhibiting function of NR5A2 was mediated via its requirement for maintenance of acinar cell fate, and upon deletion of *NR5A2*, these cells acquire a duct-like metaplastic state. Likewise, in the nervous system, NR5A2 regulates binary fate decisions by specifically promoting neuronal cell fate at the expense of astroglial cell types or neural progenitor cells (17). Considering that glioblastoma cells are originating from either progenitor or astroglial cells, it is particularly tempting to speculate that the ability of NR5A2 to inhibit these cell fates in favor of neuronal identity may contribute to suppressing the onset of glioblastoma and/or other tumors of the nervous system. In agreement, we have previously reported that NR5A2 is sufficient and necessary to promote neuronal identity via direct induction of *Prox1* gene expression (17). Here, we show that Prox1 is also induced by NR5A2 in the context of human glioblastoma and neuroblastoma cells and that it is sufficient to exert antitumor actions in glioblastoma cells. We have also previously reported a tumor-inhibiting function for Prox1 in neuroblastoma cells (42). These data support a scenario where the NR5A2-Prox1 regulatory axis prevents tumorigenesis in the nervous system by both suppressing proliferation and also promoting neuronal identity at the expense of other cell fates that can form a potential pool of tumor-initiating cells. Furthermore, a recently published study revealed an additional antitumorigenic action of NR5A2 in the pancreatic tissue, which is mediated through transcriptional repression of proinflammatory genes and pathways (67). Mechanistically, the authors showed that NR5A2, in the pancreas, directs a transcriptional regulatory network toward induction of a cell differentiation program, but in the absence or heterozygosity of *NR5A2*, this network switches and promotes inflammation instead of differentiation, thus highly increasing the risk of developing cancer (67). A similar mechanism may be operating in the nervous system since we have also reported that targeted ablation of NR5A2 in the early CNS, first, severely impairs neuronal differentiation and, second, induces a large number of proinflammatory genes, including members of the JAK-STAT pathway as well as *C1qb*, *C3ar1*, *C5ar1*, and *Cxcl18* genes (17), which were also reported to be induced in the pancreas in an Nr5a2 down-regulation–dependent manner (67).

Despite the notion that these observations suggest a tumor-preventing function of NR5A2 in the pancreas and nervous system, a number of reports indicate its involvement in cancer progression and promotion of proliferation in other cell types, tissues,

and organs. In particular, it has been previously shown that NR5A2 positively controls proliferation of colon, gastric, breast, and liver cancer cells (26, 28–30, 33–38). These data highlight the complexity and context-dependent actions of NR5A2 in cancer pathogenesis and cell cycle regulation. In the case of colon and breast cancer, NR5A2 promotes the proliferation by inducing the expression of Cyclin D1 (encoded by *CCND1* gene). Of note, despite the strong antiproliferative effect of NR5A2 on glioblastoma cells, it is also able to promote the expression of the *CCND1* gene. However, in glioblastoma cells, NR5A2 exerts additional actions by enhancing expression of $p21^{Cip1}$ and $p27^{Kip1}$, which probably manage to counteract the effect of elevated levels of Cyclin D1 on proliferation and further block cell cycle progression. This hypothesis is supported by the fact that $p21^{Cip1}$ and $p27^{Kip1}$ negatively regulate cell cycle progression via their ability to directly inactivate the CDKs/Cyclin D1 complexes. In addition, the context-dependent oncogenic role of NR5A2 in other organs may be explained by its inability to induce $p21^{Cip1}$ and $p27^{Kip1}$, therefore allowing Cyclin D1 to promote cell cycle progression. The molecular mechanism by which a nuclear receptor could employ multiple and, in some cases, opposing regulatory effects on different cell types may be explained by differential interactions with a large number of binding partners and thus differential control of downstream target genes. In agreement, NR5A2 has been previously reported to interact with many coactivators, corepressors, or other transcription factors in a cell-type specific manner, including CTNNB (beta catenin), PGC-1a, CBP, CREB1, FXR, MBF1, SRC1/3, NRIP1, SMARCD3, SMRT, SHP, DAX1, and Prox1 (19, 68). Thus, NR5A2 may be able to affect cell cycle genes and either promote or inhibit them depending on the cellular and/or developmental context.

Taken together, in this study, we have unveiled a tumor-inhibiting function of NR5A2 and its agonists in nervous system–related cancer cells. Our data render NR5A2 as a target gene for future therapeutic strategies against glioblastoma.

Materials and Methods

A detailed description of the materials and methods can be found in *SI Appendix*.

Ethics Statement. The study protocol was approved by the local ethics committee (Athens Prefecture Veterinarian Service; K3237/11-05-2012) and took place in the animal facilities of the Center for Experimental Surgery of the Biomedical Research Foundation of the Academy of Athens. All animals were handled in strict accordance with good animal practice as defined by the relevant European and Greek animal welfare bodies.

Cell Culture and Transfection Methods. All cells were cultured in a 37 °C humidified incubator with 5% CO_2 (details in *SI Appendix*).

Immunostainings. For the cell-immunostaining experiments, all cell lines and primary cells were cultured onto poly-L-lysine (Sigma) coated coverslips in 24-well plates. Detailed procedures and information of the antibodies are provided in *SI Appendix*.

RNA Extraction and Real-Time RT-qPCR Analysis. Total RNA was isolated from cells and tissues with TRI reagent solution (AM9738, Ambion/RNA, Life Technologies) according to the manufacturer's instructions followed by treatment with RQ1 DNase (Promega). Detailed procedures and information of the primers are provided in *SI Appendix*.

Immunoblotting. Total protein was isolated from cells with lysis buffer RIPA. The homogenates were centrifuged at 17,000*g* for 10 min at 4 °C. Detailed procedures and information of the antibodies are provided in *SI Appendix*.

Luciferase Assay. Luciferase-reporter assays were performed with luciferase/β galactosidase kits (Promega) (42, 44, 69, 70). For the *p21*-Luc, *p27*-Luc, and *Prox1*-Luc construct, we have used 0.5 μg per transfection per well (cells plated in 12-well plates at a density of 2×10^5) and 1.5 μg of pEYFP-LRH1 or pCAGGS-GFP and 0.15 μg of a β-galactosidase expression plasmid to normalize for transfection efficiency.

Flow Cytometry and Cell Cycle-Cell Death Assessment. Detailed methods, procedures, and information of the antibodies are provided in *SI Appendix*.

ChIP Experiments. To analyze the molecular interactions of NR5A2 in the nervous system, ChIP experiments were carried out in U87-MG cells. Detailed procedures and information about primer sets are provided in *SI Appendix*.

The sequences of the core consensus response element for NR5A2 (NR5A2RE) were identified on each promoter sequence using the Gene Transcription Regulation Database (71) and Eucaryotic Promoter Database (https://epd.epfl.ch//index.php). The primers sequences are presented in the following list:

Allotransplantation Experiments (Xenografts). Heterotopic and orthotopic xenografts were performed as previously reported (42) and described in details in the *SI Appendix*. In all cases, the DLPC group was treated with a daily dose of 100 mg of DLPC per kg of mouse weight (100 mg/kg), as previously reported to be an efficient and nontoxic dose to the animals (47). The coordinates for orthotopic xenografts relative to bregma is: −1.5 mm anteroposterior, +1.5 mm mediolateral from the bregma, and −2.5 mm dorsoventral from the surface of the skull, according to the mouse stereotaxic atlas (72).

LC-HRMS Determination of DLPC. Mice were treated with DLPC for 3 d with a daily dose of 100 mg/kg. The mice from the control group were treated with the solvent of DLPC. DLPC and vehicle were administered orally using a gavage device. After treatment, the mice were killed and brains were isolated and proceeded to lipid extraction. Specifically, lipids of 1 g brain tissue were extracted using methanol chloroform method (Folch method) (73). The samples were then prepared for LC-HMRS. LC-HRMS experiments were carried out using a Triple TOF 4600 (ABSciex) coupled with a micro-LC (Eksigent), an autosampler set at 5 °C and a thermostated column compartment, in the positive electrospray ionization mode. A Halo C18 2.7 μM, 90 Å, 0.5 × 50 mm column (Eksigent) was employed for the chromatography at a flow rate of 55 μL/min, and the mobile phases A and B were consistent of acetonitrile/0.01% formic acid/isopropanol 80/20 vol/vol and water/0.01% formic acid, respectively. The elution gradient started with 5% of phase B for 0.5 min, gradually increasing to 98% in the next 7.5 min. These conditions were maintained for 0.5 min, and then the column was re-equilibrated (at the initial conditions) for 1.5 min. MultiQuant 3.0.2 and PeakView 2.1 (ABSciex) were used for data acquisition and processing. The EICs were obtained with the use of MultiQuant 3.0.2, which created the base peak chromatograms for the masses that achieve a 0.01 Da mass accuracy width. The relative tolerance of the retention time was set within a margin of ±2.5%. Three samples of animal brain were analyzed per condition by LC-HRMS.

Experimental Design and Statistical Analysis. All experimental designs are explained in each part of the *Materials and Methods*. The normal distribution of values was verified with the Shapiro–Wilk normality test using IBM SPSS Statistics for Windows, Version 20.0. To ensure the reproducibility of results, all experiments were performed independently three to four times. For statistical analysis, all measurements and experimental values from independent experiments were estimated with two-tailed Student's *t* test. All the results are shown as mean ± SD. The exact *P* values are described in each figure legend. P values < 0.05 are considered statistically significant. All analyses were done using GraphPad 8 and Microsoft Excel 2013.

Data Availability. All study data are included in the article and/or the *SI Appendix*.

ACKNOWLEDGMENTS. We thank I. Talianidis, A. Charonis, A. Papadimitropoulou, D. Pefani, M. Xilouri, and T. Rampias for supplying plasmids, antibodies, and experimental tools. We thank C. Flytzanis, P. Katsoris, A. Michail, M. Tsampoula, E. Ninou, V. Kaltezioti, G. Barkas, D. Antoniou, and N. Malissovas for technical advice and discussions. We would also like to acknowledge the excellent technical assistance and guidance by Anna Agapaki with histological analysis of the mouse brain tumors. This work was supported by the Hellenic Foundation for Research and Innovation (H.F.R.I.) under the "First Call for H.F.R.I. Research Projects to support Faculty members and Researchers and the procurement of high-cost research equipment grant" (Project Number: 1782) as well as ARISTEIA-II (NeuroNetwk, No.4786) and Fondation Santé Biomedical Research grants (to P.K.P.).

1. S. Karcher *et al*., Different angiogenic phenotypes in primary and secondary glioblastomas. *Int. J. Cancer* **118**, 2182–2189 (2006).
2. J. Wang, C. Bettegowda, Genomic discoveries in adult astrocytoma. *Curr. Opin. Genet. Dev.* **30**, 17–24 (2015).
3. K. Urbańska, J. Sokołowska, M. Szmidt, P. Sysa, Glioblastoma multiforme - An overview. *Contemp. Oncol. (Pozn.)* **18**, 307–312 (2014).
4. H. G. Wirsching, E. Galanis, M. Weller, Glioblastoma. *Handb. Clin. Neurol.* **134**, 381–397 (2016).
5. L. Caja, C. Bellomo, A. Moustakas, Transforming growth factor β and bone morphogenetic protein actions in brain tumors. *FEBS Lett.* **589**, 1588–1597 (2015).
6. J. M. Maris, M. D. Hogarty, R. Bagatell, S. L. Cohn, Neuroblastoma. *Lancet* **369**, 2106–2120 (2007).
7. A. D. Pearson *et al*.; European Neuroblastoma Study Group; Children's Cancer and Leukaemia Group (CCLG formerly United Kingdom Children's Cancer Study Group), High-dose rapid and standard induction chemotherapy for patients aged over 1 year with stage 4 neuroblastoma: A randomised trial. *Lancet Oncol.* **9**, 247–256 (2008).
8. D. S. Nørøxe, H. S. Poulsen, U. Lassen, Hallmarks of glioblastoma: A systematic review. *ESMO Open* **1**, e000144 (2017).
9. H. Zong, R. G. Verhaak, P. Canoll, The cellular origin for malignant glioma and prospects for clinical advancements. *Expert Rev. Mol. Diagn.* **12**, 383–394 (2012).
10. A. Chaurasia, S. H. Park, J. W. Seo, C. K. Park, Immunohistochemical analysis of ATRX, IDH1 and p53 in glioblastoma and their correlations with patient survival. *J. Korean Med. Sci.* **31**, 1208–1214 (2016).
11. A. Moustakas, T. N. Kreisl, New treatment options in the management of glioblastoma multiforme: A focus on bevacizumab. *OncoTargets Ther.* **3**, 27–38 (2010).
12. C. L. Tso *et al*., Distinct transcription profiles of primary and secondary glioblastoma subgroups. *Cancer Res.* **66**, 159–167 (2006).
13. J. E. Visvader, Cells of origin in cancer. *Nature* **469**, 314–322 (2011).
14. A. L. Vescovi, R. Galli, B. A. Reynolds, Brain tumour stem cells. *Nat. Rev. Cancer* **6**, 425–436 (2006).
15. S. Alcantara Llaguno *et al*., Cell-of-origin susceptibility to glioblastoma formation declines with neural lineage restriction. *Nat. Neurosci.* **22**, 545–555 (2019).
16. S. Alcantara Llaguno *et al*., Malignant astrocytomas originate from neural stem/progenitor cells in a somatic tumor suppressor mouse model. *Cancer Cell* **15**, 45–56 (2009).
17. A. Stergiopoulos, P. K. Politis, Nuclear receptor NR5A2 controls neural stem cell fate decisions during development. *Nat. Commun.* **7**, 12230 (2016).
18. E. Fayard, J. Auwerx, K. Schoonjans, LRH-1: An orphan nuclear receptor involved in development, metabolism and steroidogenesis. *Trends Cell Biol.* **14**, 250–260 (2004).
19. S. Stein, K. Schoonjans, Molecular basis for the regulation of the nuclear receptor LRH-1. *Curr. Opin. Cell Biol.* **33**, 26–34 (2015).
20. M. C. Meinsohn, O. E. Smith, K. Bertolin, B. D. Murphy, The orphan nuclear receptors steroidogenic factor-1 and liver receptor homolog-1: Structure, regulation, and essential roles in mammalian reproduction. *Physiol. Rev.* **99**, 1249–1279 (2019).
21. J. L. Mamrosh *et al*., Nuclear receptor LRH-1/NR5A2 is required and targetable for liver endoplasmic reticulum stress resolution. *eLife* **3**, e01694 (2014).
22. K. A. Lazarus, D. Wijayakumara, A. L. Chand, E. R. Simpson, C. D. Clyne, Therapeutic potential of Liver Receptor Homolog-1 modulators. *J. Steroid Biochem. Mol. Biol.* **130**, 138–146 (2012).
23. D. Gkikas, M. Tsampoula, P. K. Politis, Nuclear receptors in neural stem/progenitor cell homeostasis. *Cell. Mol. Life Sci.* **74**, 4097–4120 (2017).
24. N. Grgurevic, S. Tobet, G. Majdic, Widespread expression of liver receptor homolog 1 in mouse brain. *Neuroendocrinol. Lett.* **26**, 541–547 (2005).
25. J. C. Heng *et al*., The nuclear receptor Nr5a2 can replace Oct4 in the reprogramming of murine somatic cells to pluripotent cells. *Cell Stem Cell* **6**, 167–174 (2010).
26. S. Bianco, M. Jangal, D. Garneau, N. Gévry, LRH-1 controls proliferation in breast tumor cells by regulating CDKN1A gene expression. *Oncogene* **34**, 4509–4518 (2015).
27. T. Ye *et al*., Nr5a2 promotes cancer stem cell properties and tumorigenesis in non-small cell lung cancer by regulating Nanog. *Cancer Med.* **8**, 1232–1245 (2019).
28. L. Liu *et al*., Nr5a2 promotes tumor growth and metastasis of gastric cancer AGS cells by Wnt/beta-catenin signaling. *OncoTargets Ther.* **12**, 2891–2902 (2019).
29. O. A. Botrugno *et al*., Synergy between LRH-1 and beta-catenin induces G1 cyclin-mediated cell proliferation. *Mol. Cell* **15**, 499–509 (2004).
30. L. Xiao *et al*., LRH-1 drives hepatocellular carcinoma partially through induction of c-myc and cyclin E1, and suppression of p21. *Cancer Manag. Res.* **10**, 2389–2400 (2018).
31. G. von Figura, J. P. Morris, C. V. Wright, M. Hebrok, Nr5a2 maintains acinar cell differentiation and constrains oncogenic Kras-mediated pancreatic neoplastic initiation. *Gut* **63**, 656–664 (2014).
32. Y. K. Banasavadi-Siddegowda *et al*., PRMT5-PTEN molecular pathway regulates senescence and self-renewal of primary glioblastoma neurosphere cells. *Oncogene* **36**, 263–274 (2017).
33. J. R. Bayrer, S. Mukkamala, E. P. Sablin, P. Webb, R. J. Fletterick, Silencing LRH-1 in colon cancer cell lines impairs proliferation and alters gene expression programs. *Proc. Natl. Acad. Sci. U.S.A.* **112**, 2467–2472 (2015).
34. A. L. Chand, K. A. Herridge, E. W. Thompson, C. D. Clyne, The orphan nuclear receptor LRH-1 promotes breast cancer motility and invasion. *Endocr. Relat. Cancer* **17**, 965–975 (2010).
35. A. L. Chand *et al*., The orphan nuclear receptor LRH-1 and ERα activate GREB1 expression to induce breast cancer cell proliferation. *PLoS One* **7**, e31593 (2012).
36. M. M. França, B. Ferraz-de-Souza, A. M. Lerario, M. C. Fragoso, C. F. Lotfi, POD-1/TCF21 Reduces SHP Expression, Affecting LRH-1 Regulation and Cell Cycle Balance in Adrenocortical and Hepatocarcinoma Tumor Cells. *BioMed Res. Int.* **2015**, 841784 (2015).
37. H. B. Kramer *et al*., LRH-1 drives colon cancer cell growth by repressing the expression of the CDKN1A gene in a p53-dependent manner. *Nucleic Acids Res.* **44**, 582–594 (2016).
38. P. Xu *et al*., LRH-1-dependent programming of mitochondrial glutamine processing drives liver cancer. *Genes Dev.* **30**, 1255–1260 (2016).
39. J. Jen *et al*., Deletion of p16 and p15 genes in brain tumors. *Cancer Res.* **54**, 6353–6358 (1994).
40. J. E. Oh *et al*., Genetic alterations in gliosarcoma and giant cell glioblastoma. *Brain Pathol.* **26**, 517–522 (2016).
41. G. F. Reis *et al*., CDKN2A loss is associated with shortened overall survival in lower-grade (World Health Organization Grades II-III) astrocytomas. *J. Neuropathol. Exp. Neurol.* **74**, 442–452 (2015).
42. I. P. Foskolou, D. Stellas, I. Rozani, M. D. Lavigne, P. K. Politis, Prox1 suppresses the proliferation of neuroblastoma cells via a dual action in p27-Kip1 and Cdc25A. *Oncogene* **32**, 947–960 (2013).
43. J. Becker, B. Wang, H. Pavlakovic, K. Buttler, J. Wilting, Homeobox transcription factor Prox1 in sympathetic ganglia of vertebrate embryos: Correlation with human stage 4s neuroblastoma. *Pediatr. Res.* **68**, 112–117 (2010).
44. V. Kaltezioti *et al*., Prox1 regulates the notch1-mediated inhibition of neurogenesis. *PLoS Biol.* **8**, e1000565 (2010).
45. C. Vignon *et al*., Flow cytometric quantification of all phases of the cell cycle and apoptosis in a two-color fluorescence plot. *PLoS One* **8**, e68425 (2013).
46. S. G. Mays *et al*., Crystal structures of the nuclear receptor, liver receptor homolog 1, bound to synthetic agonists. *J. Biol. Chem.* **291**, 25281–25291 (2016).
47. J. M. Lee *et al*., A nuclear-receptor-dependent phosphatidylcholine pathway with antidiabetic effects. *Nature* **474**, 506–510 (2011).
48. R. J. Whitby *et al*., Identification of small molecule agonists of the orphan nuclear receptors liver receptor homolog-1 and steroidogenic factor-1. *J. Med. Chem.* **49**, 6652–6655 (2006).
49. S. G. Mays *et al*., Development of the first low nanomolar liver receptor homolog-1 agonist through structure-guided design. *J. Med. Chem.* **62**, 11022–11034 (2019).
50. P. M. Musille *et al*., Antidiabetic phospholipid-nuclear receptor complex reveals the mechanism for phospholipid-driven gene regulation. *Nat. Struct. Mol. Biol.* **19**, 532–537 (2012).
51. M. Tsampoula *et al*., Nuclear receptor NR5A2 promotes neuronal identity in the adult hippocampus. *Mol. Neurobiol.* **58**, 1952–1962 (2021).
52. C. Out *et al*., Liver receptor homolog-1 is critical for adequate up-regulation of Cyp7a1 gene transcription and bile salt synthesis during bile salt sequestration. *Hepatology* **53**, 2075–2085 (2011).
53. I. N. Krylova *et al*., Structural analyses reveal phosphatidyl inositols as ligands for the NR5 orphan receptors SF-1 and LRH-1. *Cell* **120**, 343–355 (2005).
54. R. J. Whitby *et al*., Small molecule agonists of the orphan nuclear receptors steroidogenic factor-1 (SF-1, NR5A1) and liver receptor homologue-1 (LRH-1, NR5A2). *J. Med. Chem.* **54**, 2266–2281 (2011).
55. H. A. Ingraham, Metabolism: A lipid for fat disorders. *Nature* **474**, 455–456 (2011).
56. Z. Shi, T. Shen, Y. Liu, Y. Huang, J. Jiao, Retinoic acid receptor γ (Rarg) and nuclear receptor subfamily 5, group A, member 2 (Nr5a2) promote conversion of fibroblasts to functional neurons. *J. Biol. Chem.* **289**, 6415–6428 (2014).
57. H. Zhong, G. Chan, Y. Hu, H. Hu, D. Ouyang, A comprehensive map of FDA-approved pharmaceutical products. *Pharmaceutics* **10**, E263 (2018).
58. S. Stein *et al*., SUMOylation-dependent LRH-1/PROX1 interaction promotes atherosclerosis by decreasing hepatic reverse cholesterol transport. *Cell Metab.* **20**, 603–613 (2014).
59. M. Schiappacassi *et al*., p27Kip1 expression inhibits glioblastoma growth, invasion, and tumor-induced neoangiogenesis. *Mol. Cancer Ther.* **7**, 1164–1175 (2008).
60. I. M. Chu, L. Hengst, J. M. Slingerland, The Cdk inhibitor p27 in human cancer: Prognostic potential and relevance to anticancer therapy. *Nat. Rev. Cancer* **8**, 253–267 (2008).
61. N. Kfoury *et al*., Cooperative p16 and p21 action protects female astrocytes from transformation. *Acta Neuropathol. Commun.* **6**, 12 (2018).
62. B. H. Choi *et al*., p21 Waf1/Cip1 expression by curcumin in U-87MG human glioma cells: Role of early growth response-1 expression. *Cancer Res.* **68**, 1369–1377 (2008).
63. E. Bergmann *et al*., Expression of P27 (KIP1) is prognostic and independent of MYCN amplification in human neuroblastoma. *Int. J. Cancer* **95**, 176–183 (2001).
64. G. M. Petersen *et al*., A genome-wide association study identifies pancreatic cancer susceptibility loci on chromosomes 13q22.1, 1q32.1 and 5p15.33. *Nat. Genet.* **42**, 224–228 (2010).
65. L. C. Murtaugh, Putting GWAS to the functional test: NR5A2 and pancreatic cancer risk. *Gut* **63**, 535–536 (2014).
66. M. Flandez *et al*., Nr5a2 heterozygosity sensitises to, and cooperates with, inflammation in KRas(G12V)-driven pancreatic tumourigenesis. *Gut* **63**, 647–655 (2014).
67. I. Cobo *et al*., Transcriptional regulation by NR5A2 links differentiation and inflammation in the pancreas. *Nature* **554**, 533–537 (2018).
68. C. Nadolny, X. Dong, Liver receptor homolog-1 (LRH-1): A potential therapeutic target for cancer. *Cancer Biol. Ther.* **16**, 997–1004 (2015).
69. V. Kaltezioti *et al*., Prox1 regulates Olig2 expression to modulate binary fate decisions in spinal cord neurons. *J. Neurosci.* **34**, 15816–15831 (2014).
70. P. K. Politis, S. Akrivou, C. Hurel, O. Papadodima, R. Matsas, BM88/Cend1 is involved in histone deacetylase inhibition-mediated growth arrest and differentiation of neuroblastoma cells. *FEBS Lett.* **582**, 741–748 (2008).
71. S. Kolmykov *et al*., GTRD: An integrated view of transcription regulation. *Nucleic Acids Res.* **49** (D1), D104–D111 (2021).
72. K. Franklin, G. Paxinos, *Paxinos and Franklin's the Mouse Brain in Stereotaxic Coordinates, Compact* (Elsevier, 2001).
73. J. Folch, M. Lees, G. H. Sloane Stanley, A simple method for the isolation and purification of total lipides from animal tissues. *J. Biol. Chem.* **226**, 497–509 (1957).
74. M. Bredel *et al*., Functional network analysis reveals extended gliomagenesis pathway maps and three novel MYC-interacting genes in human gliomas. *Cancer Res.* **65**, 8679–8689 (2005).